INL/CON-08-14131
PREPRINT

A CFD M&S Process for Fast Reactor Fuel Assemblies

Experiments and CFD Code Applications to Nuclear Reactor Safety (XCFD4NRS 2008)

Kurt D. Hamman
Ray A. Berry

September 2008

A CFD M&S PROCESS FOR FAST REACTOR FUEL ASSEMBLIES

Kurt D. Hamman and Ray A. Berry

Idaho National Laboratory
P.O. Box 1625
Idaho Falls, Idaho, 83415-3840, USA

Abstract
A CFD modeling and simulation process for large-scale problems using an arbitrary fast reactor fuel assembly design was evaluated. Three dimensional flow distributions of sodium for several fast reactor fuel assembly pin spacing configurations were simulated on high performance computers using commercial CFD software. This research focused on 19-pin fuel assembly “benchmark” geometry, similar in design to the Advanced Burner Test Reactor, where each pin is separated by helical wire-wrap spacers. Several two-equation turbulence models including the k-ε and SST (Menter) k-ω were evaluated. Considerable effort was taken to resolve the momentum boundary layer, so as to eliminate the need for wall functions and reduce computational uncertainty. High performance computers were required to generate the hybrid meshes needed to predict secondary flows created by the wire-wrap spacers; computational meshes ranging from 65 to 85 million elements were common. A general validation methodology was followed, including mesh refinement and comparison of numerical results with empirical correlations. Predictions for velocity, temperature, and pressure distribution are shown. The uncertainty of numerical models, importance of high fidelity experimental data, and the challenges associated with simulating and validating large production-type problems are presented.

1. INTRODUCTION

With global energy consumption expected to increase by over 50% by the year 2030, there has been an international effort to design and build advanced nuclear power plants capable of providing a safe, clean, and sustainable energy supply. Given the underlying programmatic, financial, and technical constraints of new designs, it is clear that building expensive prototypes is not practical; therefore, modeling and simulation (M&S) will be relied upon throughout the nuclear power plant life-cycle management process. Streamlined M&S processes and computing system productivity improvements will be key success factors in meeting project cost and schedule commitments, including design objectives, for international and domestic energy initiative programs.

In an effort to meet programmatic goals, recent advances in technology and the need for high fidelity computational data have resulted in research efforts focused on the integration of multi-physics phenomena and the development of new and improved numerical solvers and physical models. These contributions are expected to significantly reduce the uncertainty and increase the accuracy of M&S tools, allowing scientists and engineers to better predict physical phenomena such as critical heat flux (CHF) and reduce the uncertainty associated with hot channel factors. Unfortunately high fidelity computational data, which implies better representation of the physical geometry, requires more computer memory, larger data storage, improvements in data management, faster data processing and transfer, and robust visualization tools.

However, minimal emphasis has been placed on the simulation of large production-type problems using state-of-the-art commercial software and hardware. Large-scale simulations have the potential of providing insight into the problems and challenges that can be expected upon implementing advanced M&S tools in production codes and on advanced HPC systems. Identifying and solving these problems early in the research phase minimizes the impact on project cost and schedule during the design and development phase of new generation nuclear power plants.

This report provides an overview of the general M&S process that was followed for this study, and then expands on the verification and validation (V&V) methodology. Primarily, methodologies and preliminary results are presented. Theoretical aspects of the commercial CFD software, for example numerical solvers and turbulence models, can be found in the STAR-CCM+ User Manual (2007) or the literature.

1.1 Purpose of Study

The purpose of this study was to investigate and evaluate a computational fluid dynamic (CFD) M&S process, which included CAD geometry development, meshing, simulation, and post-processing of results, for large problems using an arbitrary fuel assembly design as a benchmark problem. Preliminary three dimensional flow distributions of sodium for several fast reactor fuel assembly pin spacing configurations were simulated using commercial CFD software and high performance computers (HPCs). This study focused on a 19-pin fuel assembly, similar in design to the Advanced Burner Test Reactor (ABTR), with wire-wrap spacers. Assembly nomenclature, consistent with that presented by Todreas and Kazimi (2001), is adhered too. Four geometric models, with different inner pin spacing and helical pitch, were developed for the study. Several two-equation turbulence models including the k-ε and SST (Menter) k-ω were evaluated. Considerable effort was taken to resolve the momentum boundary layer, so as to eliminate the need for wall functions. High performance computers were required to generate the hybrid meshes needed to predict secondary flows created by the helical wire-wrap spacers; computational meshes ranging from 65 to 85 million elements were common. A general validation methodology, which included examining iterative convergence, consistency, spatial convergence, temporal convergence, comparison of CFD results with experimental data, and examining model uncertainties was followed (NPARC Alliance, 2008). Additionally, a speed-up curve was developed to help assess computational productivity. Predictions for velocity, temperature, and pressure distribution are shown. The uncertainty of numerical models, importance of high fidelity experimental data, HPC productivity, and the challenges associated with simulating and validating large production-type problems are discussed.

2. MODELING AND SIMULATION

The M&S process was comprised of a four phases which included creating a solid-model using commercial CAD software, generating a computational mesh and running the simulation on high performance computers (HPCs) using commercial CFD software, and conducting rudimentary validation studies using dated empirical correlations published in the literature. Lessons-learned from scoping studies of a single-pin and a three-pin assembly were incorporated into the analysis.

Commercial software was used for this study because of its robustness, functionality, and ability to provide quick-turnaround solutions for a wide range of problems. The ability to import a wide range of CAD files, select different meshing models, numerical solver and turbulence model selection, and post-processing capabilities provides the CFD practitioner with a versatile toolset for modeling and simulation. For example, the geometric complexities created by modeling the wire-wrap spacers made the use of less sophisticated solid modeling techniques impractical. The CAD software provided the capability to automate the model allowing fuel assembly geometric design changes to be made quickly. This was important when evaluating modeling tradeoffs because several geometric design changes were required before a computational mesh of sufficient quality was obtained. Finally having quick access to several turbulence models was advantageous, especially when conducting sensitivity analysis studies.

2.1 CAD Model

A computer aided design (CAD) solid model of a 19 pin fuel assembly was created using SolidWorks, commercial software (SolidWorks, 2008). The software was automated with geometric equations and terminology consistent with that presented by Todreas and Kazimi (2001). For example, geometric parameters and terminology such as "clearance per interior pin - Δp", "flat-to-flat tolerance - T", and "the fraction of assembly tolerance distributed within the rods - F" were adhered too. Four geometric models were developed for this study. Models M(1) thru M(3) were developed for the preliminary isothermal hydrodynamic simulation which included a turbulence model analysis and wire-wrap geometric model sensitivity analysis, and model M(4) was developed for the HTFF analysis. Models M(1) thru M(3) were 20 cm in length with a helical pitch of 20.3 cm, and model M(4) was 20.3 cm in length with a helical pitch of 20.3 cm. Table 1 presents the geometric details of each model, including the ABTR geometry; a description of the geometry is shown in Figure 1.

Table 1: Geometric Model Parameters

Model	Pins	D	D_s (3)	P/D	P	ΔP	Δg	D_{ft}	D_l	Length	T (2)	F (2)
ABTR	217	0.800	0.103	1.130	0.904	0.001	0.033	13.598	-	260	0.0797	0.174
M(1)	19	0.800	0.103	1.169	0.936	0.039	0.032	4.299	2.482	20.0	0.2001	0.675
M(2)	19	0.800	0.103	1.149	0.919	0.023	0.016	4.210	2.431	20.0	0.1113	0.708
M(3)	19	0.800	0.103	1.135	0.908	0.012	0.005	4.148	2.395	20.0	0.0498	0.799
M(4)	19	0.800	0.103	1.127	0.902	0.005	0.005	4.126	2.382	20.3	0.0273	0.634

Notes:

1. All dimensions in centimeters.

2. Assembly geometry based on Todreas and Kazimi, where "T" represents the flat-to-flat tolerance and "F" represents the fraction of assembloy tolerance distributed within the rods.

3. Model geometry includes a pin-to-wirewrap overlap of 0.0065 cm

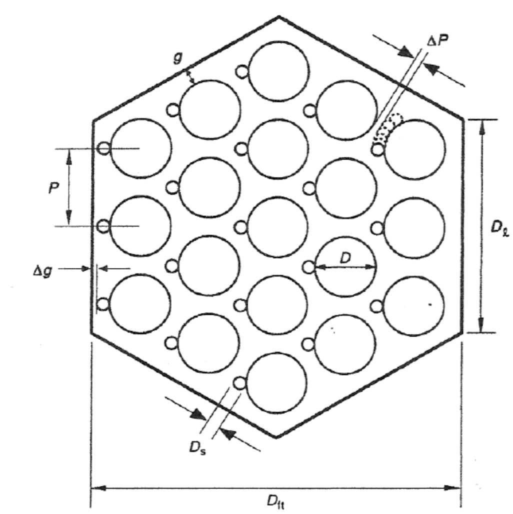

Todreas, N.E. & Kazimi, M.S., Nuclear Systems II, Elements of Thermal Hydraulic Design, Taylor and Francis, 2001.

Fig. 1: 19-Pin Fast Reactor Geometry Description.

The fuelpin solid model and computational volume are shown in Figures 2 and 3. The rotation direction of the spacer wire is clockwise when viewed from the rod-bundle outlet, Figure 3. Although the fuelpin solid geometry could have been modeled together with the computational fluid volume, for example a conjugate heat transfer analysis, the number of mesh elements would have been prohibitive for preliminary scoping studies. During the CAD phase, wire-wrap geometric models shown in Figures 4 were evaluated. Although wire-wrap models “B” and “C” are simple to mesh and result in fewer numbers of elements, they do not accurately represent the physical geometry, adding to simulation uncertainty. Knowing that wire-wrap model “A” would better represent the physical geometry, but at the expense of more computational elements, this geometry was chosen for the study.

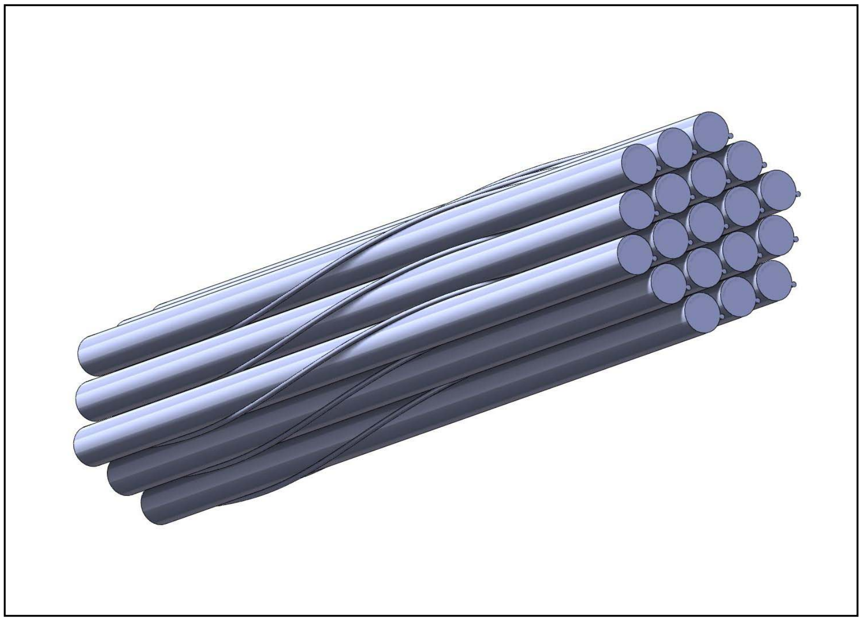

Fig. 2: 19-Pin Fast Reactor Solid Model.

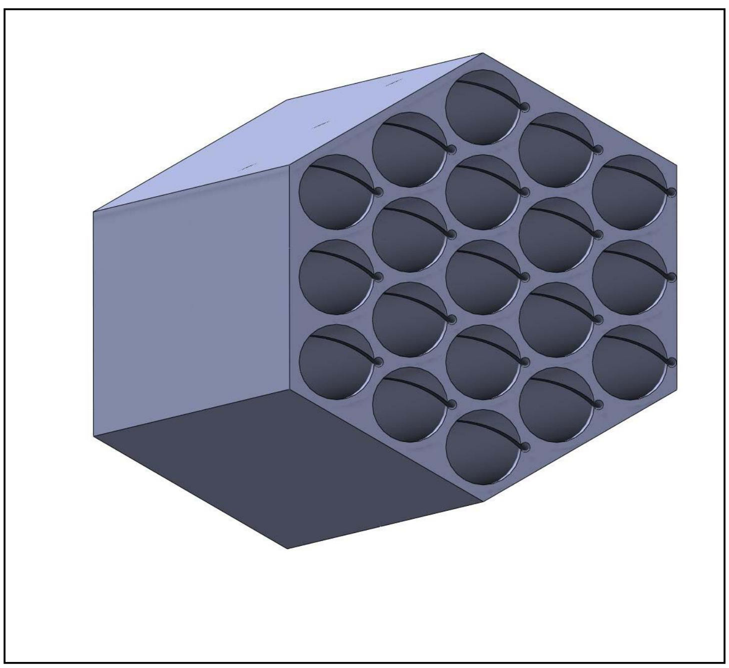

Fig. 3: Computational Fluid Volume (outlet face).

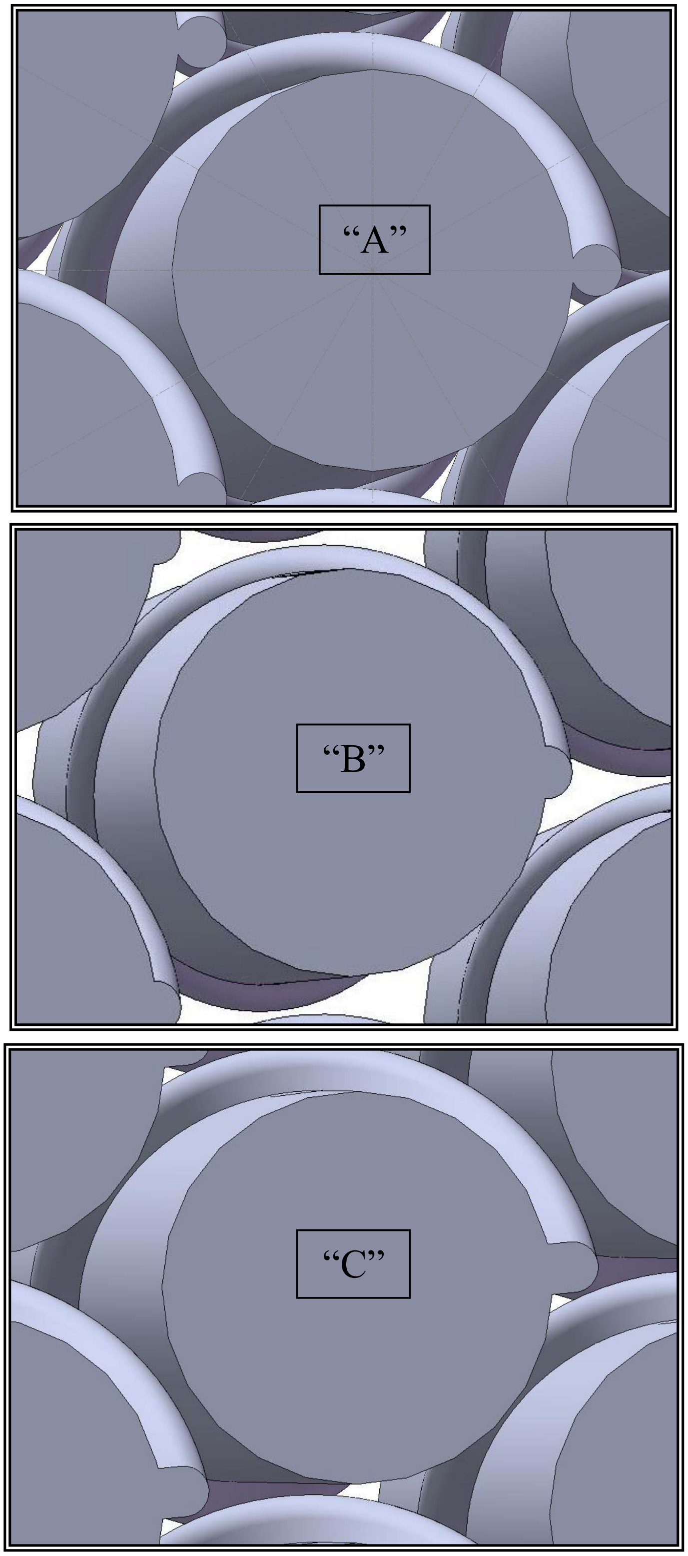

Fig. 4: Wire-Wrap Geometric Models "A", "B", and "C"

The CAD geometry was exported from the parent software package in a parasolid format. This CAD format was found to ensure a good quality surface mesh and no geometric scaling. For example upon import into the CFD software, some CAD formats will scale the dimensions of the solid model geometry.

2.2 Mesh Generation

Several meshers were evaluated for this study. The mesh generator chosen for this study is classified as an automated unstructured serial mesher (STAR-CCM+, 2007). Three meshing models were used: surface remesher, prism layer mesher, and a polyhedral mesher. Using the surface mesh imported with the CAD geometry, which in general is of poor quality, the surface remesher creates a surface mesh of improved quality. A good quality volume mesh depends on a surface mesh free of errors with good quality elements. The prism layer mesher creates the hydrodynamic boundary layer elements necessary to resolve the momentum boundary layer; the wide range of length scales within the computational domain makes generating the boundary layer extremely difficult (Figure 1). The polyhedral mesher was chosen for this study since polyhedral elements are known to be more accurate than tetrahedral elements with a comparable number of cells (CD-adapco, 2008).

Computational requirements for meshing the geometry were significant. Contributing to this was the complex geometry and the desire to predict the complex fluid flow created by the wire-wraps. Because the commercial software did not have parallel meshing capabilities and meshing required between 65 GB and 85 GB of memory, the mesh was generated on a SGI Altix 4700 shared memory machine with 256 GB of memory and Intel Itanium 2 processors with a 1.5 GHz clock speed. Close coordination between other researchers accessing the HPC was important in order to ensure sufficient memory was continuously available during the meshing process. Approximately 24 to 48 hours were required to generate each computational mesh; so mesh generation scoping studies, designed to establish correct mesh setpoints, were performed on scaled geometries prior to attempting meshing on the larger models.

The full-scale 3-D simulation consisted of 65 million hybrid elements for models M(1) thru M(3) and 85.5 million hybrid elements for model M(4). Although the use of wall functions would have reduced the number of mesh elements required at wall boundaries, considerable effort was taken to resolve the momentum boundary layer in order to minimize the need for wall functions and reduce simulation uncertainty. In short, a challenging geometry and problem was chosen for this study.

The mesh is shown in Figures 5 and 6. In Figure 5, note the dense areas of mesh elements where the fuelpin wire-wraps approach the wrapper wall; contour color was added to better show the concentration of mesh elements. The impact of geometry containing sharp corners is shown in Figure 6 where the wire-wrap intersects the fuelpin. Obtaining a good quality mesh in this region proved to be challenging.

2.3 Simulation Solver and Models

The following simulation settings and models were used for the vertically oriented fuel assembly: 3-D, incompressible flow, SST (Mentor) k-ω turbulence model with "all y+ wall treatment" for geometric models M(1) thru M(3) and "low y+ wall treatment" for geometric model M(4), steady-state segregated solver, using second order upwind convection schemes. Since the flow is incompressible (with the gravity model "enabled"), coupling between the momentum equation and energy equation is established using the Boussinesq approximation. Material properties for sodium at 700K were used (Fink, 1995). This temperature is near the average coolant temperature of the ABTR (Chang, 2006).

The segregated solver was chosen because it requires less memory than a coupled solver; a "rule-of-thumb" for this CFD software is that for every 1 million mesh elements, the segregated solver requires 1 GB of memory and the coupled solver requires 2 GB of memory. The SST (Mentor) k-ω turbulence model was chosen based on preliminary sensitivity analysis results presented in section 3.6 of this paper. The "all y+ wall treatment" was chosen based on the recommended guidance provided in the CFD software user manual, but the wall treatment was changed to "low y+" for model C(4) for scoping study purposes. The default turbulence parameters, 0.01 for turbulence intensity and 10 for turbulent viscosity, were retained for all simulations.

Inlet temperature was specified at 680K; inlet velocity was specified at 2 m/s. A static pressure of 0 psi was specified at the outlet. For the HTFF analysis, a constant heat flux of approximately 1 MW/m^2 was applied at the fuelpin boundaries and adiabatic conditions were specified at the wrapper wall. Inlet velocity of 2 m/s was chosen to ensure that turbulent flow would exist within the computational domain (Cheng, 1986); Reynolds number based on hydraulic diameter for the HTFF simulation was 19,200.

The primary HPC used to run the simulations was a SGI Altix ICE 8200 distributed memory machine with 2048 compute cores, 8 cores/node, 16 GB/node, and containing quad-core Intel Xeon "Clovertown" processors with a 2.66 GHz clock speed. The simulation file size ranged from 22.1 GB to 27.5 GB and the simulation memory requirements ranged from 65 GB to 85 GB. Simulation time was approximately 10 days using 256 processors.

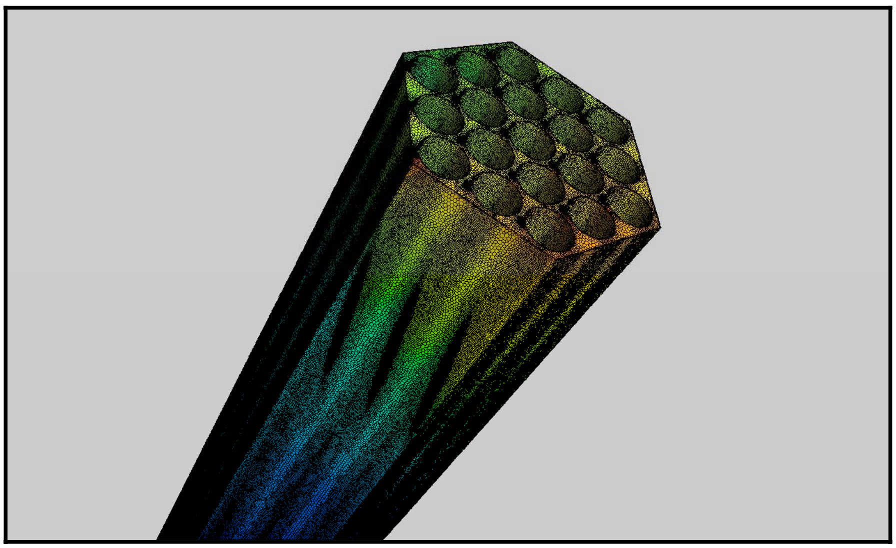

Fig. 5: Fuel Assembly Mesh (outlet face shown)

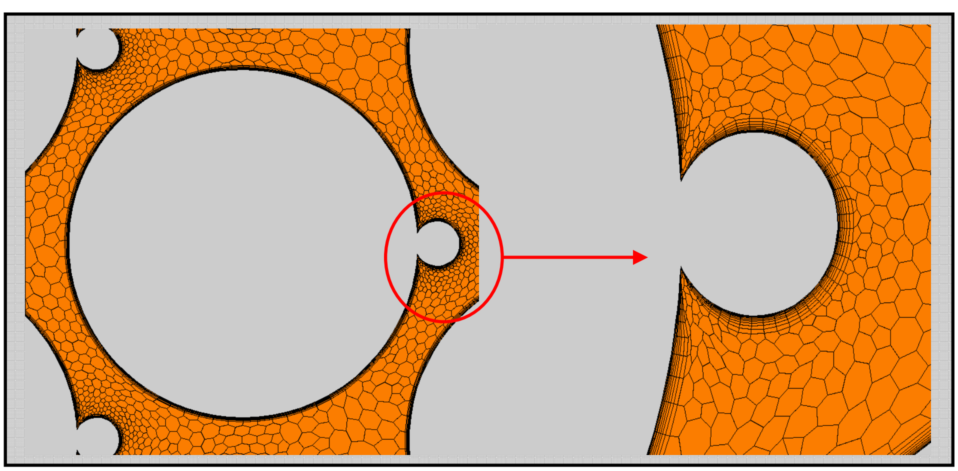

Fig. 6: Center Fuelpin Mesh (showing boundary layer)

2.4 Post Processing Data

All post processing of the results was performed with the geometry partitioned and a dedicated head node. Post processing of the results proved to be difficult for the entire assembly, especially if the mesh was enabled; specifically, the graphics were slow to respond. The reason for this slow response is unknown; but it could be the result of network infrastructure bandwidth limitations, software limitations, or the magnitude of the simulation problem size. Therefore, analysis of the results primarily was restricted to specific faces and planes. Figures 7 thru 12 show the results from the HTFF simulation using model M(4).

Figure 7 shows that large velocity and thus large mass flowrates are observed in the edge sub-channels; physically, the larger flowrates are the result of larger flow areas in these sub-channels. Figure 8 is a vector velocity plot with velocity vectors projected tangent to the plane. This figure shows the complex secondary flows that are developed as the result of the wire-wraps and the momentum boundary layer. Figure 9 shows the pressure distribution at the inlet face near a wire-wrap. Given that the wire-wraps rotate clockwise with respect to the outlet planes, the low pressure side of the wire-wrap is consistent with the results presented in the contour plot. The highest pressure is predicted at the fuelpin and wire-wrap interface. It is not clear whether or not this high pressure is physical; however, it is speculated that the high pressure is the result of the sharp angle at the fuelpin and wire-wrap interface. Figure 10 shows the axial pressure distribution on an arbitrary face; the simulation does not predict any localized low pressure areas, which if present could indicate the potential for exceeding fuelpin thermal limits. Consistent with the velocity distribution plots, the temperature distribution plots, shown in Figures 11 and 12, predict that the highest temperatures exist in the fuel assembly interior subchannels, near the regions between the fuelpin and an adjacent wire-wrap, suggesting the need for a design change which would result in a more uniform flow throughout the assembly. Note the high temperature region, shown in Figure 12, between the inner fuelpin and adjacent fuelpin wire-wrap which follows the outline of the wire-wrap, suggesting the presence of localized hot spots.

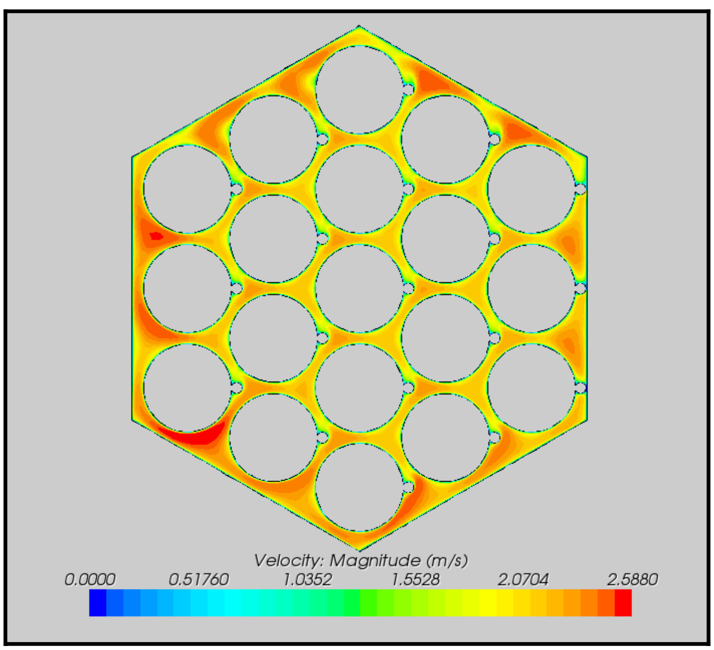

Fig. 7: Velocity Magnitude (outlet face)

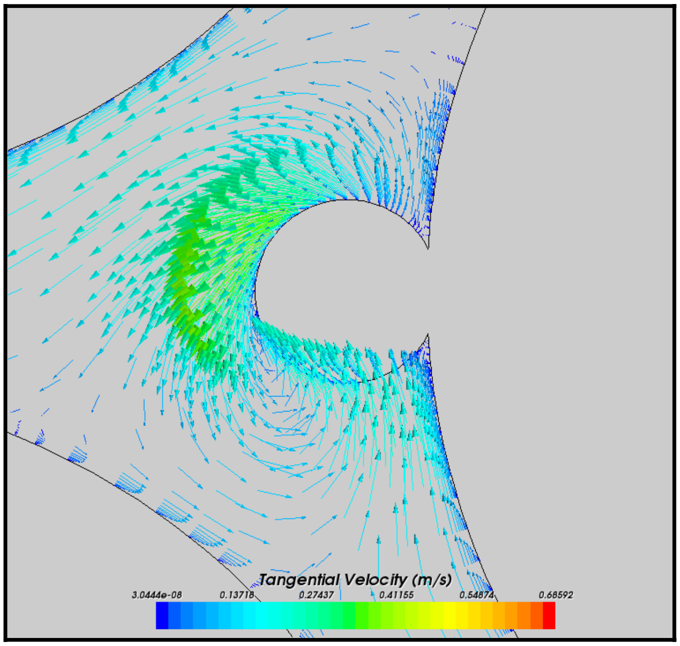

Fig. 8: Vector Velocity Plot (midplane face)

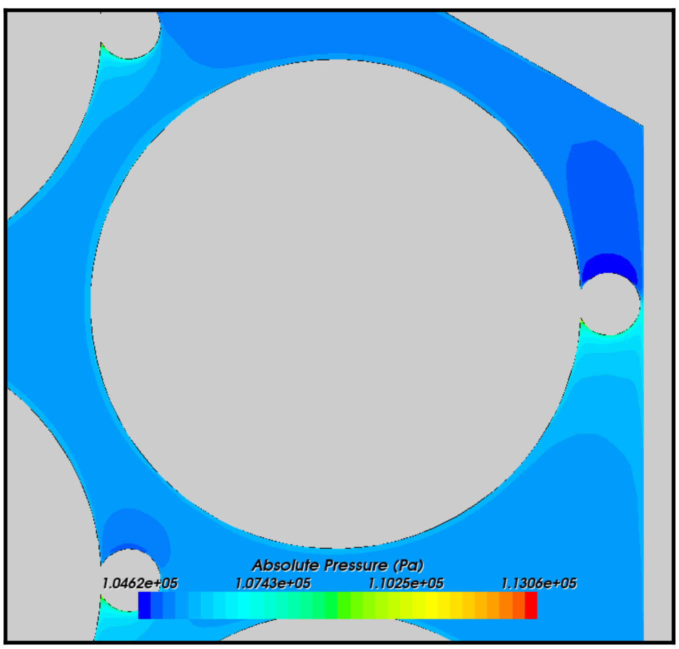

Fig. 9: Local Pressure Distribution (inlet face)

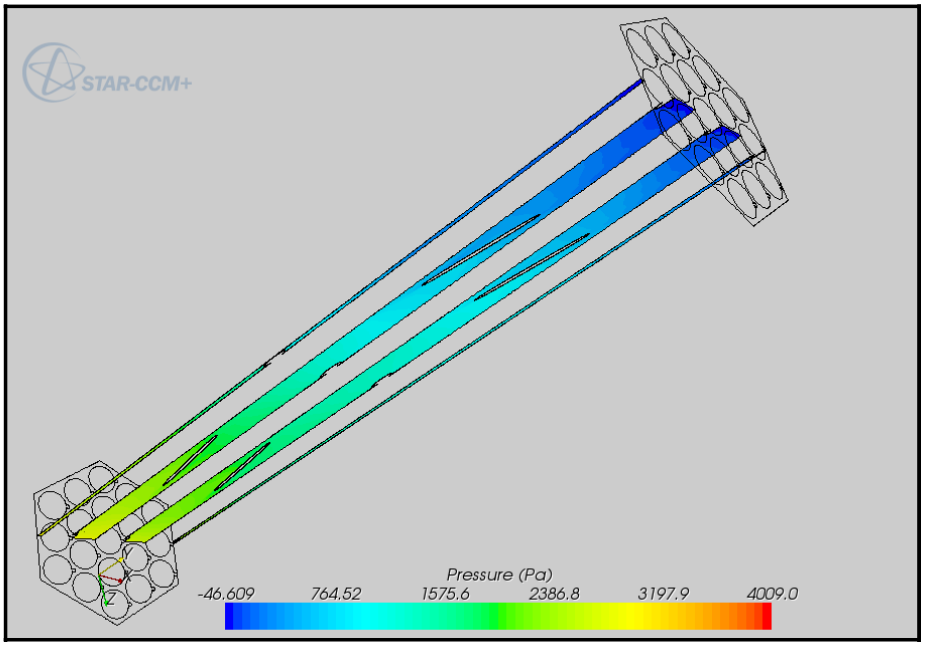

Fig. 10: Axial Static Pressure Distribution

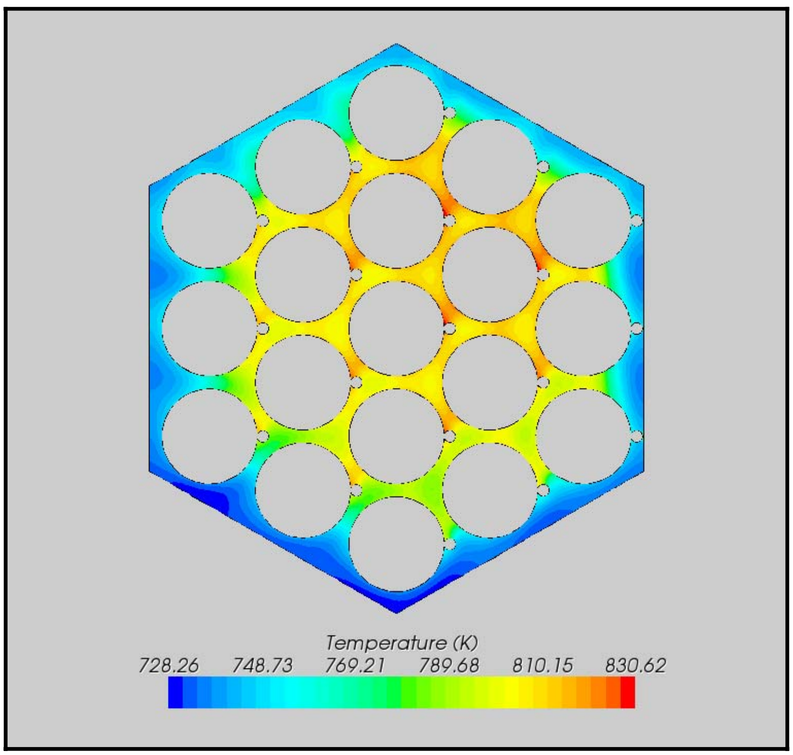

Fig. 11: Temperature Contours (outlet face)

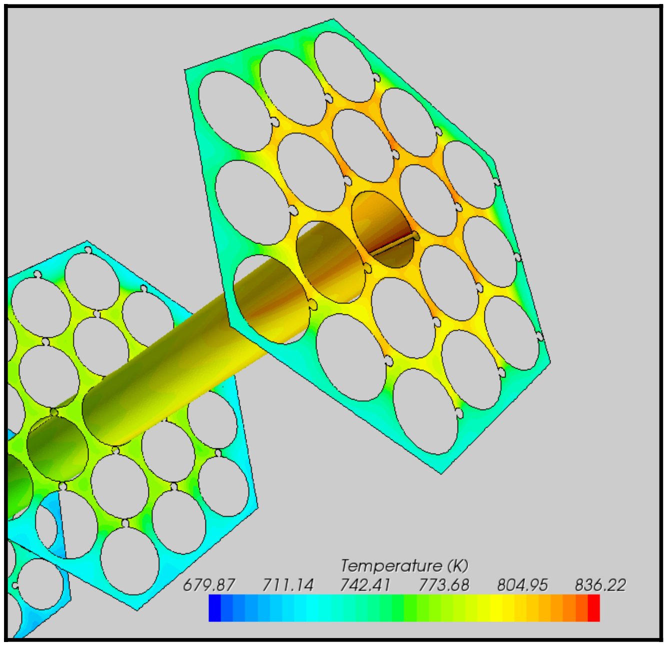

Fig. 12: Temperature Contours (axial faces)

3. VERIFICATION AND VALIDATION

One of the most difficult and important steps of the M&S process is establishing the credibility of the numerical results. Although verification is an important step in the V&V process, the responsibility for software verification primarily resides with the commercial code vendors. Validation, determining that the results of the simulation are an accurate representation of the real world, primarily resides with the CFD practitioner (AIAA, 2002). Several professional societies and researchers have published V&V literature, but to date only V&V "guidelines" have been agreed upon. The V&V methodology followed in this study was obtained from the NPARC Alliance (2008).

3.1 Examine Iterative Convergence

Steady-state conditions and convergence were based on the behaviour of transport equation residuals. Figure 13 shows the iterative convergence history. The CFD simulation results were obtained by first conducting an isothermal hydrodynamic analysis until steady-state conditions were reached; using the isothermal hydrodynamic results, the final steady-state HTFF results were obtained using the segregated energy solver. As shown, residuals were reduced by 4 to 6 orders of magnitude. The large amount of "numerical noise" observed in the behaviour of the turbulent kinetic energy and turbulent dissipation rate residuals is noted. The reason for this behaviour is being evaluated.

3.2 Examine Consistency

In this study, simulation consistency was evaluated by monitoring mass and energy quantities. Plots of net mass flowrate and net heat transfer are shown in Figures 14 and 15. The net mass flowrate curve is flat and the net heat transfer curve increases at a decreasing rate until the curve eventually flattens; this behaviour suggests that steady state has been reached. Net mass flowrate reaches a value of zero, while net heat transfer reaches a value of 20 watts, which is 0.002% of the total power input. Noteworthy is that heat transfer converged at a different rate than the residuals in Figure 13, emphasizing the importance of judging simulation convergence using other metrics beside residuals.

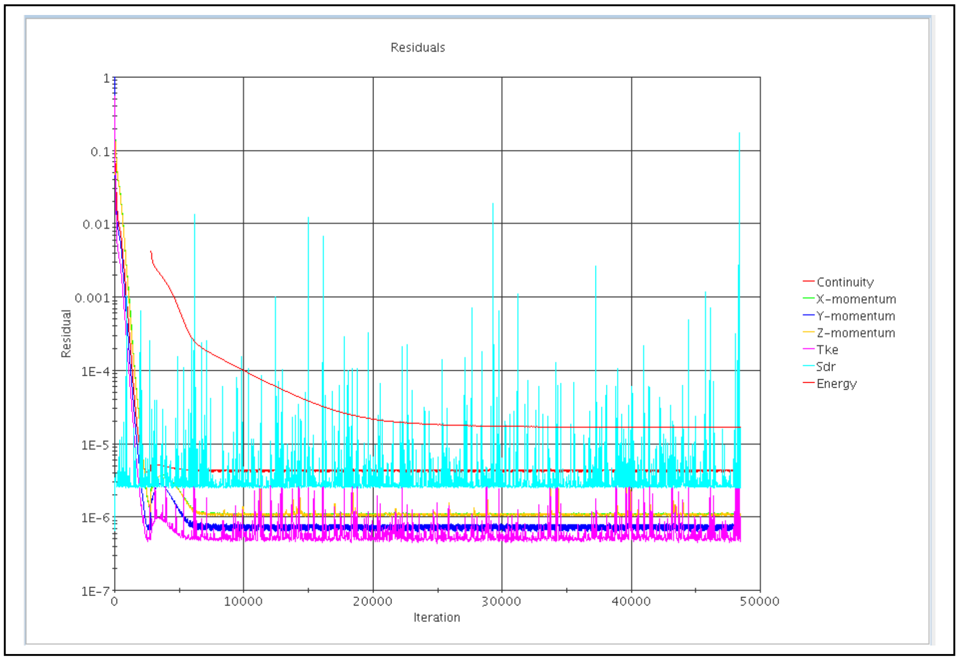

Fig. 13: Iterative Convergence Graph

3.3 Examine Spatial Convergence

Typically, one assumes that spatial (i.e. grid) convergence has been achieved after running the simulation on successively finer grids until a negligible change in the important dependent variables are observed (AIAA, 2002); grid coarsening techniques can be used as well (NPARC Alliance, 2008). In this study, mesh refinement attempts were made; but in the end, a software limitation, previously unknown, restricted mesh sizes to approximately 100 million elements.

Figure 16 is a graph of several plots of memory usage required by the commercial mesher on the SGI Altix 4700. The green plot shows the memory requirements required to generate a 65.5 million element mesh ("Successful Mesh"). The blue plot is the memory usage during an attempt to create a 65.5 million element mesh, but insufficient memory prevented mesh generation since other researchers were accessing a large portion of the HPC memory. The red plot is the memory usage during several meshing attempts in which a "Vector Reserve Error" was encountered. This error eventually was isolated to a software limitation. This error limited hybrid (i.e. prism layer and polyhedral elements) meshes to approximately 100 million elements. Therefore, efforts to examine spatial convergence were postponed. Recently, this problem was resolved; and software cell count capabilities of approximately 250 million elements are expected.

Nevertheless, establishing spatial convergence for large production type problems with an unstructured hybrid mesh will be challenging; furthermore, simulating complex reactor components with a wide range of geometric length scales will contribute to these challenges. Although a significant amount of research, primarily focused on structured meshes, has been performed for computational meshes; insufficient guidance, with a sound technical foundation, has been provided to CFD practitioners who simulate large complex geometry problems on hybrid unstructured meshes. This shortcoming suggests the need for high fidelity experimental data and a computational process to evaluate and quantify "localized" numerical uncertainty.

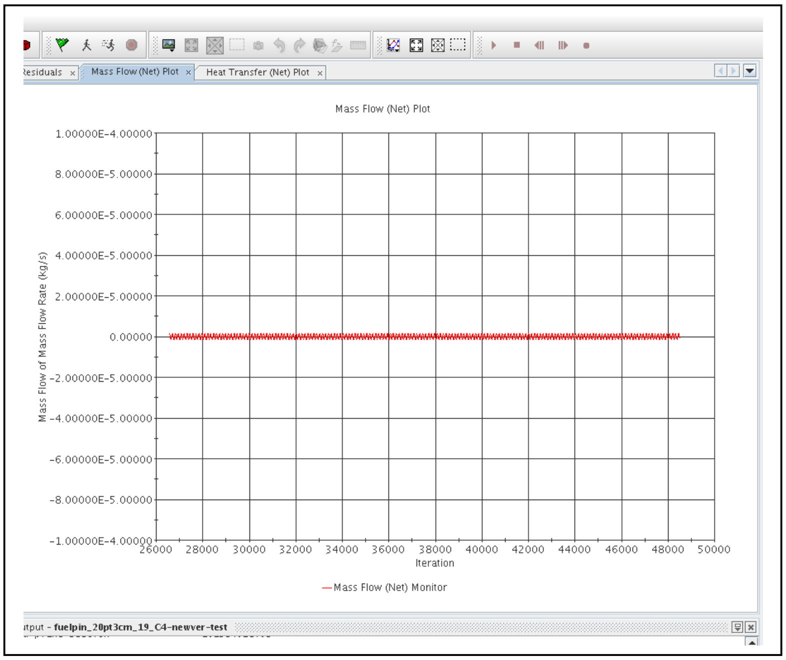

Fig. 14: Net Mass Flowrate

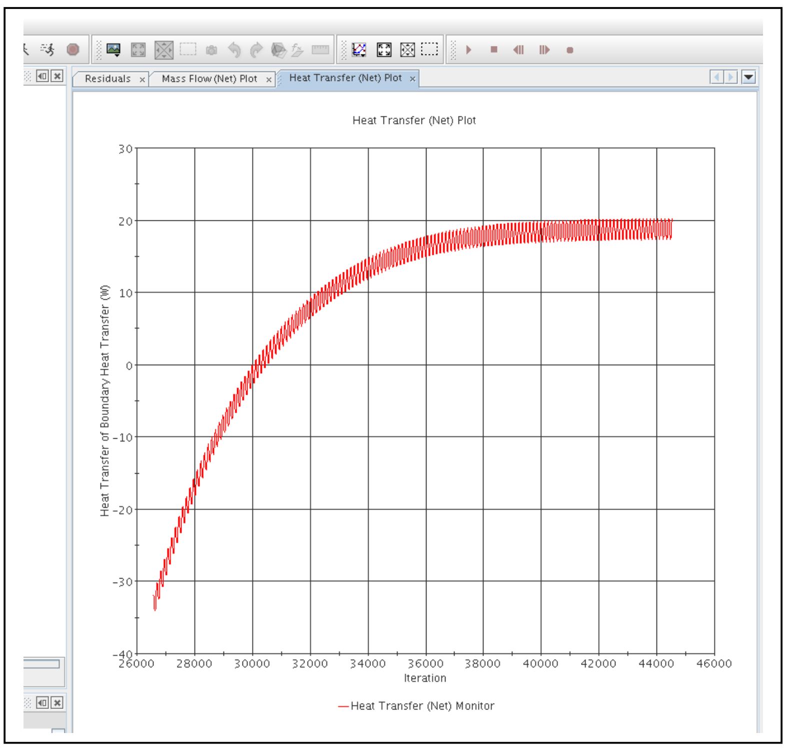

Fig. 15: Net Heat Transfer

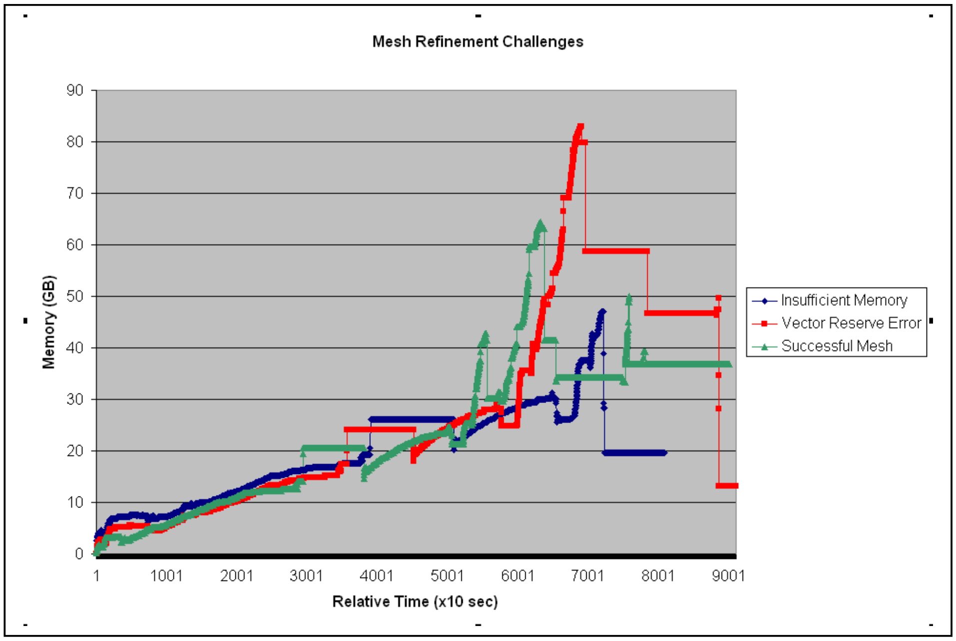

Fig. 16: Meshing Memory Requirements

3.4 Examine Temporal Convergence

Temporal convergence was not assessed since a steady-state problem was simulated. Nevertheless, the challenges a conducting a temporal convergence study should be addressed. Given that the file size for the 85 million element problem was 27.5 GB and the steady-state solution required approximately 10 days to complete, transient convergence studies would require significant computational time and huge amounts of disk storage space. This suggests a need for a parallel I/O capability.

3.5 Comparison with Experimental Data

As a rudimentary first step in validation of the simulation results, average "global" pressure results were compared with Rehme's (1973) empirical correlation and Novendstern's (1972) empirical correlation. Average pressure across the inlet face was computed and used to determine axial pressure drop across the midplane of the assembly. The CFD simulation predicted a pressure drop of 156 Pa/cm, while Rehme's correlation predicted a pressure drop of 136 Pa/cm (9% difference) and Novendstern's correlation predicted a pressure drop of 172 Pa/cm (15% difference). Such close agreement between the simulation and the empirical correlations is encouraging in that it provides the CFD practitioner with a sense that the global pressure results provided by the simulation are reasonable, but "global" comparisons by themselves are insufficient for simulation validation. Additionally, recognize the small differential pressures (200 Pa/cm $\approx$ 0.03 psi/cm) analyzed in this study.

Although researchers have shown interest in producing experimental data for wire wrap geometries (Fernandez, 2000 and McCreery, 2008), insufficient high fidelity experimental data exists for validation studies; therefore, comparison of "localized" numerical results with high fidelity experimental data was not performed for this particular geometry and HTFF conditions.

3.6 Examine Model Uncertainties

The uncertainty associated with turbulence models and wire-wrap geometry models was evaluated. Two hydrodynamic sensitivity analysis studies, for several assembly configurations, were performed. The first study evaluated turbulence model performance for several interior pin-clearance geometries M(1), M(2), M(3) described in Table 1; the second study evaluated assembly pressure drop using different wire-wrap geometric models (A, B, C). Each analysis focused on an assembly, similar in design to the ABTR assemblies. Shown in Figures 17 and 18 are the results of the sensitivity analysis studies.

Figure 17 shows CFD results plotted with data produced from published empirical correlations. Note that the numerical pressure drop analyzed does not include hydrostatic pressure effects. Empirical correlations were used since experimental data of the quality necessary for code validation was not available. The realizable k-ε turbulence model agreed well with data produced using Novendstern's empirical correlation, while the SST (Menter) k-ω turbulence model showed good agreement with Rehme's empirical correlation. Residual convergence problems were observed with model M(3). These problems were believed to be the result of smaller pin clearances (i.e. Δp and Δg).

Figure 4 presented the wire-wrap geometric models studied. Although model "A" better represents the actual geometry, creating this computational mesh proved to be challenging. Mesh generation for models "B" and "C" were not difficult. Figure 18 compares pressure drop results from empirical correlations and CFD results. Noteworthy is that the pressure drop predicted using model "A" closely approximated the pressure drop predicted using Rehme's correlation.

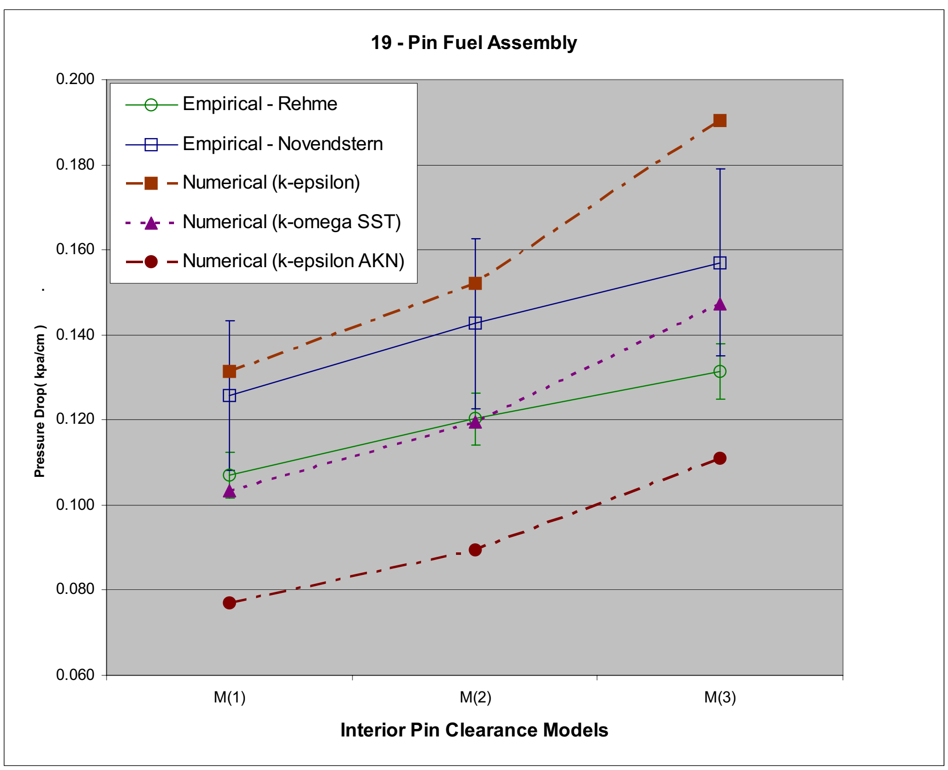

Fig. 17: Sensitivity Analysis – Turbulence Models

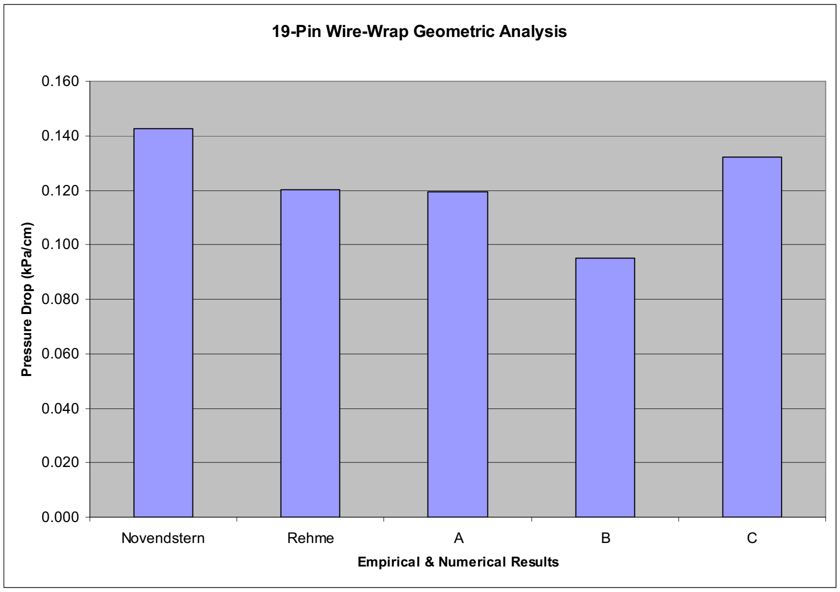

Fig. 18: Sensitivity Analysis Results – Wire-wrap Models

4. HPC PRODUCTIVITY

Consistent with program cost and schedule requirements, HPC productivity should be assessed for large-scale simulations. "The measurement of productivity for a particular user on a particular system with a particular application is a difficult question that must encompass a variety of concepts." (Kepner, 2004) One particular productivity metric which characterizes the integral hardware/software efficiency is a speedup curve. Speedup curves should be developed when it is expected that numerous large-scale production simulations will be run. Speedup metrics provide CFD practitioners and project managers with a realistic estimate of simulation times and computational productivity, and they also can be used to identify hardware and software problems.

Therefore a speed-up curve was developed using STAR-CCM+ V3.02.003 on an SGI Altix ICE 8200 distributed machine with dedicated computational nodes (i.e. 8 procs per compute node with one dedicated head node for I/O) and the geometric model M(1). Figure 19 presents the results of the speedup analysis. The linear curve represents "ideal" conditions in which the use of N processors reduces total computational time by a factor of 1/N. The blue curve, which depends on several factors including hardware, software, and physics models, is the "real" performance curve (Knight, 2003). Note that linear behaviour is observed for up to approximately 128 processors, and that computational efficiency reduces if more than 512 processors are used. The decrease in computational efficiency is the result of increased communication between nodes as the number of processors increases.

The commercial CFD software performs automatic partitioning of the computational domain. Partitioning for the speedup test was based on the original 64 partition simulation. For example, the 256 partition simulation was created beginning with the 64 partition simulation. Post testing discussions with the commercial software vendor indicate that using a single partition as the base partition is expected to provide better load balancing for the processors; speedup testing was not re-performed to evaluate load balancing effects. Additionally, due to HPC operational commitments, only one-time calculation (using 500 iterations for each run) was used to develop the curve; no other processes were accessing the computational nodes.

Noteworthy is the impact that hardware architecture has upon HPC productivity. For example, the speedup results below were performed using processor dedicated nodes. But, it was observed that when the number of nodes was doubled keeping the processor count the same, the total computation time decreased by approximately 30%. This suggests that operating the HPC at 50% of rated "processor capacity," improves computational performance by 30%. This observation is believed to be the result of quad-core bandwidth and/or cache limitations (Song, 2007).

5. CONCLUSIONS AND FUTURE WORK

Large-scale M&S problems have unique challenges that are not typically experienced during research code and model development. For example, CFD practitioners simulating problems comparable to those presented in this work should expect large file sizes, significant HPC memory requirements, long mesh generation times, and data visualization challenges. Other researchers have noted similar challenges (Gajapathy, 2007).

Conducting scoping calculations by simulating large problems can identify potential hardware and software problems that may not otherwise be identified during the simulation of small problems. Prior to beginning large-scale simulations, CFD practitioners should have an understanding of the capabilities and limitations of computational resources. But, throughout the M&S process, expect additional capabilities and limitations to be identified.

Preliminary results of the CFD studies reveal that hydrodynamic parameters, such as pressure drop, depend on turbulence models, interior pin-clearances, and wire-wrap geometric configurations. For example, wire-wrap geometric simplification results in pressure differences on the order of 20%.

Simulation validation proved to be challenging since few empirical correlations were available and high fidelity experimental data for the geometry and HTFF conditions simulated was not available. The results of this study suggest a need for high fidelity experimental data for code validation; and the long meshing times suggest a need for commercial parallel meshers.

Plans for future studies include modeling the solid fuelpins and performing detailed thermal/hydraulic CFD sensitivity analyses of the 19-pin fast reactor assembly with a heat flux profile consistent with that of the ABTR.

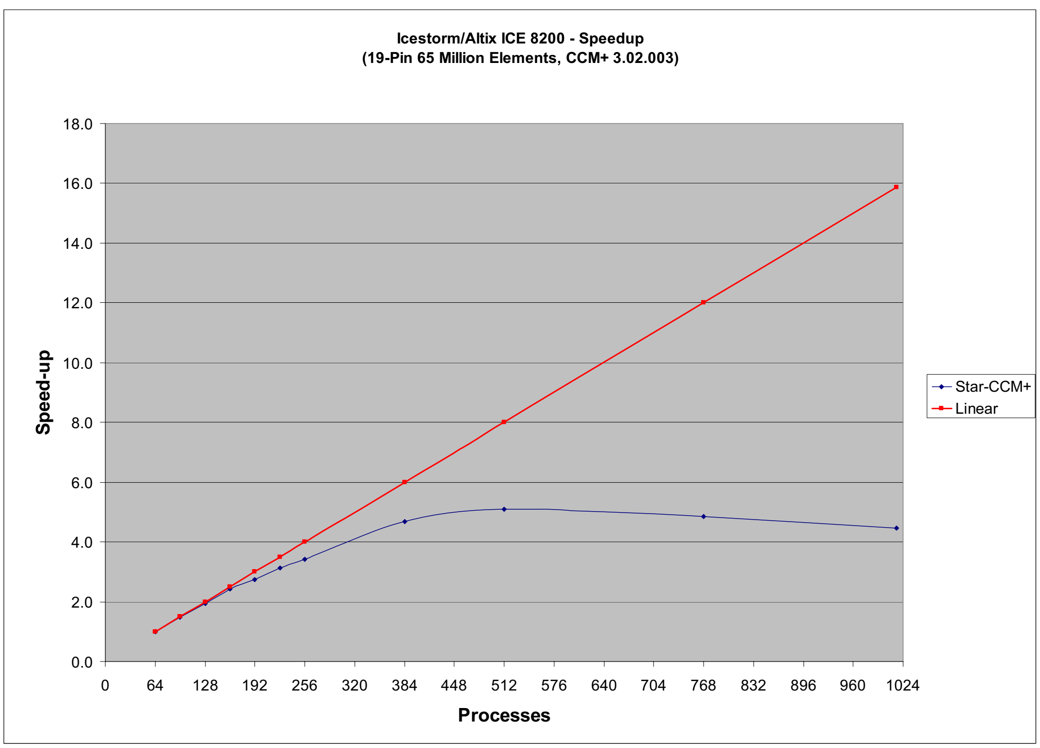

Fig. 19: Speedup Curve

REFERENCES

AIAA, *Guide for the Verification and Validation of Computational Fluid Dynamics Simulations (AIAA G-077-1998)*, AIAA, Reston, New York, USA, 2002.

CD-adapco, "The Advantage of Polyhedral Meshes," available on the Internet (accessed 4/12/08) at www.cd-adapco.com/press_room/dynamics/24/testVspoly.html .

E.F. Fernandez, E.F. and P. Carajilescov, "Static Pressure and Wall Shear Stress Distributions in Air Flow in a Seven Wire-Wrapped Rod Bundle," *Journal of the Brazilian Society of Mechanical Sciences*, 22, (2000).

E.H. Novendstern, "Turbulent Flow Pressure Drop Model for Fuel Rod Assemblies Utilizing a Helical Wire-Wrap Spacer System," *Nuclear Engineering and Design*, 22, pp. 19-27, (1972).

F. Song, S. Moore, and J. Dongarra, "L2 Cache Modeling for Scientific Applications on Chip Multi-Processors," 2007 International Conference on Parallel Processing (ICPP07), Xi'an, China, September 2007.

G.E. McCreery, et al., "Design of Wire-Wrapped Rod Bundle Matched Index-of-Refraction Experiments," Proceedings of the 16th International Conference on Nuclear engineering ICONE16," May 11-15, 2008.

J.K. Fink and L. Leibowitz, *Thermodynamic and Transport Properties of Sodium Liquid and Vapor,* ANL/RE-95/2, Chicago, Illinois, USA, January 1995.

J. Kepner, "HPC Productivity: An Overarching View," *International Journal of High Performance Computing Applications*, 18, 4, pp. 393-397 (2004).

K. Knight, et al., "High Performance Computing CFRD Final Technical Report," INL/EXT-08-14212, January 2003.

K. Rehme, "Pressure Drop Correlations for Fuel Element Spacers," *Nuclear Technology*, 17, 15, (1973).

N.E. Todreas and M.S. Kazimi, *Nuclear Systems II, Elements of Thermal Hydraulic Design*, Taylor and Francis, Boca Raton, Florida, USA, 2001.

NPARC Alliance, "Validation Assessment," available on the Internet (accessed 11/1/07) at www.grc.nasa.gov/www/wind/valid/map.html .

R. Gajapathy, et al., CFD investigation of helical wire-wrapped 7-pin fuel bundle and the challenges in modeling full scale 217 pin bundle, *Nuclear Engineering and Design*, 237, pp. 2332-2342 (2007).

S. Cheng and N.E. Todreas, "Hydrodynamic Models And Correlations For Bare And Wire-Wrapped Hexagonal Rod Bundles-Bundle Friction Factors, Subchannel Friction Factors And Mixing Parameters", *Nuclear Engineering and Design*, 92, pp. 227-251 (1986).

STAR-CCM+, Version 3.02.003, CD-adapco, New York New York, USA, 2007.

SolidWorks 2008, SolidWorks Corporation, www.solidworks.com .

Y.I. Chang, P.J. Finck, and C. Grandy, *Advanced Burner Test Reactor Preconceptual Design Report,* ANL-ABR-1, Chicago, Illinois, USA, 2006.